The Effect of Nitroglycerin on Myocardial Blood Flow in Various Segments Characterized by Rest-Redistribution Thallium SPECT

Eiji Tadamura, MD, PhD[1]; Marcelo Mamede, MD[1]; Shigeto Kubo, MD[1]; Hiroshi Toyoda, MD, PhD[1]; Masaki Yamamuro, MD[1]; Hidehiro Iida, PhD[2]; Nagara Tamaki, MD, PhD[3]; Kazunobu Nishimura, MD, PhD[4]; Masashi Komeda, MD, PhD[4]; and Junji Konishi, MD, PhD[1]

[1]Department of Nuclear Medicine and Diagnostic Imaging, Kyoto University Graduate School of Medicine, Kyoto, Japan; [2]Department of Investigative Radiology, National Cardiovascular Center, Suita, Japan; [3]Department of Nuclear Medicine, Hokkaido University School of Medicine, Sapporo, Japan; and [4]Department of Cardiovascular Surgery, Kyoto University Graduate School of Medicine, Kyoto, Japan

The use of nitrates is reported to be effective in viability detection in scintigraphic perfusion imaging. The purpose of the study was to evaluate the effect of nitroglycerin (NTG) on myocardial blood flow (MBF) and coronary vascular resistance (CVR) in various segments characterized by rest-redistribution ^{201}Tl SPECT. **Methods:** Twenty-three patients with coronary artery disease underwent rest-redistribution ^{201}Tl SPECT and ^{15}O-labeled water PET at rest and after NTG spray (0.3 mg). In addition, 11 healthy volunteers were also studied using PET. **Results:** NTG did not change global MBF in the volunteers or in the patients. In segments with normal ^{201}Tl uptake and in those with a severe irreversible ^{201}Tl defect, NTG significantly reduced MBF without changing CVR. NTG reduced CVR in segments with a reversible ^{201}Tl defect (141 ± 50 to 114 ± 29 mm Hg/[mL/min/g], $P = 0.004$) and in those with a mild-to-moderate irreversible ^{201}Tl defect (165 ± 64 to 149 ± 60 mm Hg/[mL/min/g], $P = 0.003$), while maintaining MBF. **Conclusion:** NTG preferentially reduces CVR in the viable myocardium with ischemia. After NTG, tracer uptake in the ischemic myocardium will be relatively increased compared with that in the nonviable and nonischemic myocardium, leading to improvements in viability detection.

Key Words: blood flow; nitroglycerin; perfusion; myocardial infarction

J Nucl Med 2003; 44:745–751

Myocardial scintigraphic perfusion imaging has long been used for the assessment of myocardial viability (*1–12*). Recently, several investigations have indicated that the use of nitrates in perfusion imaging is effective in the detection of viable myocardium and for prognostic assessment (*13–20*). However, few data are available on the absolute change in myocardial blood flow (MBF) after nitrates in the ischemic and the nonischemic human myocardium. Using PET, therefore, we have investigated the effect of nitroglycerin (NTG) on MBF in the various segments characterized by ^{201}Tl rest-redistribution SPECT in patients with coronary artery disease. In addition, we have also used PET to measure flow in healthy human subjects at rest and after NTG spray to examine the effect of NTG on global MBF.

MATERIALS AND METHODS

Subjects

Twenty-three patients with angiographically proven coronary artery disease who were recruited in our department for a viability assessment were consecutively studied. Sixteen of the patients had experienced a previous myocardial infarction that occurred at least 2 mo before the study. The clinical characteristics of each patient are provided in Table 1.

All patients underwent rest–4-h ^{201}Tl SPECT and PET flow quantification at rest and after a lingual NTG spray. These 2 studies were performed within 1 wk, during which time the condition of the patients was stable. All cardiac medications, except sublingual NTG, were discontinued for at least 48 h before the study. In addition, 11 healthy male volunteers (mean age, 25 ± 5 y) were studied with PET at rest and after NTG spray. None of the volunteers had a history of diabetes, hypertension, cardiovascular disease, or smoking. Entrance criteria included normal heart rate, normal blood pressure, and normal resting and stress electrocardiography (ECG) findings. Written informed consent was obtained from each subject before the study, which had been approved by the Kyoto University Ethics Committee.

PET Imaging

Each subject was positioned in the gantry of the PET camera (Advance; General Electric Medical Systems) with the aid of ultrasound. The characteristics of this camera have been described previously (*21*). The spatial resolution of the reconstructed clinical PET images is ~8 mm in full width at half maximum at the center of the field of view, and the axial resolution is ~4 mm (*21*).

A 10-min transmission scan using 2 rotating ^{68}Ge pin sources was made for the attenuation correction. After a transmission scan,

Received Jul. 8, 2002; revision accepted Oct. 31, 2002.

For correspondence or reprints contact: Eiji Tadamura, MD, Department of Nuclear Medicine and Diagnostic Imaging, Kyoto University Graduate School of Medicine, 54 Shogoinkawahara, Sakyo-ku, Kyoto, 606-8507, Japan.
E-mail: et@kuhp.kyoto-u.ac.jp

TABLE 1
Clinical Characteristics of Patients

Patient no.	Age (y)	Sex	LVEF (%)	History of MI	Coronary stenosis			Collateral vessels
					RCA	LAD	LCX	
1	84	M	35	+	90	90	75	
2	80	M	43	+	90	90	0	
3	71	M	62	−	100	90	100	LAD → RCA, LAD → LCX
4	74	M	56	−	0	90	0	
5	50	F	40	+	100	90	99	RCA → RCA
6	53	F	51	−	100	99	100	RCA → RCA, RCA → LAD, LCX → LCX
7	57	M	60	−	75	75	90	
8	76	M	30	+	0	90	0	
9	73	M	32	+	75	90	75	
10	61	M	47	+	0	75	90	
11	74	F	39	+	90	99	90	
12	59	M	42	+	100	99	50	
13	55	M	50	+	50	90	90	
14	55	M	50	+	0	90	75	
15	64	M	23	+	100	99	99	
16	57	M	37	+	100	90	75	LAD → RCA
17	73	M	41	+	0	90	75	
18	76	M	36	+	0	90	90	
19	77	M	40	+	0	75	90	
20	64	M	61	−	90	75	0	
21	76	F	55	−	90	75	90	
22	72	M	60	−	50	75	50	
23	69	M	46	+	90	99	90	
Mean	67.4		45.0					
SD	9.8		10.8					

LVEF = left ventricular ejection fraction; MI = myocardial infarction; RCA = right coronary artery; LAD = left anterior descending coronary artery; LCX = left circumflex artery.

the subjects were asked to inhale ^{15}O-CO for 2 min. After inhalation, carbon monoxide was allowed to combine with hemoglobin in red blood cells for 3 min before a 4-min static scan was started. During the scan, 3 blood samples were drawn at 2-min intervals and the radioactivity in these samples was measured. Ten minutes were allowed for decay of ^{15}O-CO radioactivity before the flow measurements. At baseline, approximately 740 MBq of ^{15}O-H_2O were injected intravenously over 2 min, and a 20-frame dynamic PET examination was performed for 6 min consisting of 6 × 5-s, 6 × 15-s, and 8 × 30-s frames (*21*). In addition, ^{15}O-H_2O was injected 5 min after lingual administration of NTG (Myocor spray, 0.3 mg; Toa Eiyo Co.) and serial images were recorded using the same sequence. All data were corrected for dead time, decay, and photon attenuation. Heart rate, arterial blood pressure, and ECG were monitored continuously during the PET studies. Heart rate and arterial blood pressure obtained during the first 4 min of each dynamic image acquisition sequence were averaged to calculate the rate–pressure product (RPP) and mean arterial blood pressure.

SPECT Imaging

For the patients, 111 MBq of ^{201}Tl were administered intravenously under resting conditions. SPECT images were acquired 15 min and 4 h after injection using a dual-head gamma camera (Millennium; General Electric Medical Systems) equipped with a high-resolution collimator (30 projections over 180°, 50 s per projection) (*22*,*23*). The first SPECT examination was performed with ECG gating (8 frames per cardiac cycle). Two energy windows were used, that is, 30% windows centered on the 70-keV peak and on the 167-keV peak.

Region-of-Interest (ROI) Definition

For each patient, measurements of regional ^{201}Tl activity and PET flow quantification were performed on the short-axis slice. The left ventricle was divided into 5 equidistant short-axis slices using the vertical long-axis image in ^{201}Tl rest-redistribution SPECT images, as shown in Figure 1. Similarly, PET data were reoriented into the short-axis plane. The extravascular density

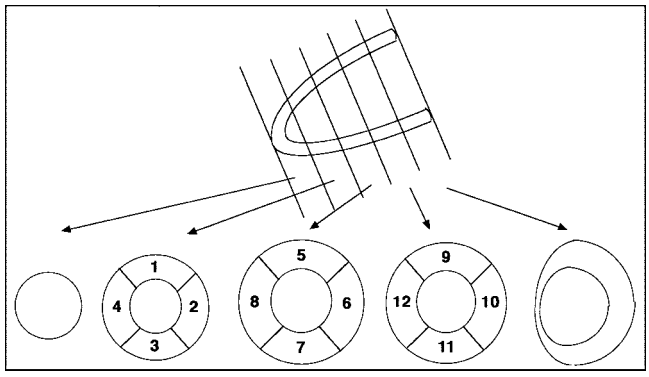

FIGURE 1. Schematic presentation of ROI definition. Twelve ROIs were determined in the 3 short-axis slices.

images and extravascular ^{15}O-H_2O images, obtained by ^{15}O-CO images, transmission images, and ^{15}O-H_2O dynamic images, were used for the delineation of the myocardium (*24*). There is a concern that edge slices of the apical and basal side may not contain a substantial amount of myocardium. When sufficient myocardium is not included in the slice, underestimation of ^{201}Tl activity is expected and PET flow quantification can be erroneous. Therefore, these slices were excluded from the analysis. Finally, 12 segments of the left myocardium, as shown in Figure 1, were analyzed in PET and SPECT studies.

SPECT Data Analysis

The left ventricular ejection fraction was obtained from the ECG-gated SPECT and a commercially available automated algorithm (Table 1) (*22*,*23*,*25*). Segment tracer activity was calculated as the total of the normalized counts of the pixels divided by the number of pixels included within the segments. The segment with maximal activity was normalized to 100, and the activity of the other segments was expressed as a percentage of the activity of the peak segment. A ^{201}Tl defect was defined when ^{201}Tl activity was $<$80% (*4*,*6*). Redistribution was defined when relative ^{201}Tl activity at 4-h imaging increased $\geq$12% above the initial value (*6*). A persistent defect at 4-h imaging was classified as mild-to-moderate when ^{201}Tl activity was $\geq$50% of maximal activity and severe when ^{201}Tl activity was $<$50% of maximal activity (*6*).

PET Data Analysis

The arterial input function was obtained from the left ventricular time–activity curve using a previously validated method in which corrections were made for the limited recovery of the left ventricular ROI and the spillover from the myocardial activities (*26*). Values of regional MBF (mL/min/g) were calculated according to the previously published method using a single-compartment model (*27*,*28*). The method we used to calculate MBF is theoretically free from the partial-volume effect or wall motion (*27*).

In addition, whole-heart MBF was determined by defining additional ROIs, each drawn to encompass the whole of the left ventricle within each image plane. To obtain global MBF, a single whole-heart time–activity curve was created by these time–activity curves, taking into account the difference in size of each ROI. Thus, whole-heart and regional values of MBF were obtained. As an index of the homogeneity of flow distribution, the coefficient of variation (COV) was derived for MBF at rest and after NTG spray. The COV was calculated as the SD divided by the mean of the whole-heart MBF values, expressed as a percentage (*24*).

To relate blood pressure as an index of coronary perfusion pressure to the blood flow, an index of coronary vascular resistance (CVR) (mm Hg/[mL/min/g]) was calculated as the ratio of mean arterial pressure to MBF (*21*,*24*,*29*).

The RPP is known to be a marker of cardiac work, which affects MBF (*29*). Therefore, MBF normalized by cardiac work was derived from the ratio of MBF (mL/min/g) to RPP (bpm $\times$ mm Hg) $\times$ 10^4.

Statistical Analysis

Statistics were calculated with a commercially available personal computer software program (StatView-J 4.5; Abacus Concepts, Inc.). Values are expressed as the mean $\pm$ SD. Differences before and after NTG were compared with Student's paired *t* test. A value of $P < 0.05$ was considered statistically significant.

RESULTS

Hemodynamic Responses to NTG

Hemodynamic data at rest and after NTG spray are shown in Table 2. Diastolic and systolic blood pressure decreased after NTG spray compared with the values at rest in patients ($P < 0.05$) and in healthy volunteers ($P < 0.05$). Heart rate increased significantly after NTG administration in patients ($P < 0.0001$) and in healthy volunteers ($P < 0.01$). The RPP did not significantly change after NTG spray in patients or in healthy volunteers.

Global MBF and CVR at Rest and After NTG

The global MBF values at rest and after NTG are also given in Table 2. Global MBF did not differ significantly at rest and after NTG in healthy volunteers (0.76 $\pm$ 0.11 vs. 0.77 $\pm$ 0.12 mL/min/g, $P = 0.845$). Global MBF tended to decrease after NTG spray, but the decrease did not show statistical significance in patients (0.80 $\pm$ 0.26 to 0.74 $\pm$ 0.23 mL/min/g, $P = 0.075$). MBF normalized by the RPP did not significantly change after NTG spray in the healthy

TABLE 2
Hemodynamic Data and Whole Left Ventricular Perfusion and Vascular Resistance at Baseline and After Nitroglycerin Spray

Parameter	Patients		Volunteers	
	Baseline	NTG	Baseline	NTG
Heart rate (bpm)	59.8 $\pm$ 8.6	65.0 $\pm$ 9.8*	59.6 $\pm$ 4.9	65.3 $\pm$ 6.2
Systolic BP (mm Hg)	131.7 $\pm$ 21.2	117.0 $\pm$ 21.8*	109.0 $\pm$ 8.0	104.0 $\pm$ 8.1
Diastolic BP (mm Hg)	77.6 $\pm$ 15.3	70.8 $\pm$ 9.1†	56.0 $\pm$ 5.6	50.5 $\pm$ 4.2
RPP (bpm $\times$ mm Hg) $\times$ 10^4	7,935 $\pm$ 1,897	7,551 $\pm$ 1,502	6,507 $\pm$ 799	6,802 $\pm$ 984
Whole-heart MBF (mL/min/g)	0.80 $\pm$ 0.25	0.74 $\pm$ 0.22	0.76 $\pm$ 0.11	0.77 $\pm$ 0.12
MBF/RPP* 10,000	1.01 $\pm$ 0.26	0.99 $\pm$ 0.26	1.09 $\pm$ 0.31	1.04 $\pm$ 0.33
Whole-heart CVR (mm Hg/[mL/min/g])	130.1 $\pm$ 39.6	126.4 $\pm$ 44.3	98.4 $\pm$ 16.3	90.4 $\pm$ 13.3

*$P < 0.0001$ vs. baseline.
†$P < 0.05$ vs. baseline.
BP = blood pressure.

volunteers (1.09 ± 0.31 to 1.04 ± 0.33 [(mL/min/g)/(mm Hg/min) × 10^4], $P = 0.490$) or in the patients (1.01 ± 0.26 to 0.99 ± 0.26 [(mL/min/g)/(mm Hg/min) × 10^4], $P = 0.537$). Moreover, global CVR was not significantly altered after NTG spray in healthy volunteers (98.4 ± 16.3 to 90.4 ± 13.3 [mm Hg/(mL/min/g)], $P = 0.149$) or in patients (130.1 ± 39.6 to 126.4 ± 44.3 [mm Hg/(mL/min/g)], $P = 0.460$).

The COV of MBF at rest and after NTG spray did not differ significantly in the healthy volunteers (10.8% ± 5.7% vs. 10.9% ± 4.5%, $P = 0.989$). In contrast, the COV of MBF decreased significantly after NTG spray in the patients (27.4% ± 9.8% to 23.6% ± 9.1%, $P = 0.016$). Thus, flow disparity among the myocardial segments was reduced after NTG spray in the patients with coronary artery disease.

SPECT Distribution Pattern in Patients

A total of 276 myocardial segments were analyzed in 23 patients. Of these, 151 (54.7%) had normal ^{201}Tl uptake, 28 (10.1%) showed a reversible ^{201}Tl defect, and 97 (35.1%) showed a fixed ^{201}Tl defect. Of the 97 fixed defects, 81 (29.3%) were mild-to-moderate and 16 (5.8%) were severe. Among the 28 segments showing a reversible ^{201}Tl defect, 2 showed a severe defect and 26 showed a mild-to-moderate ^{201}Tl defect in the initial rest images.

Regional MBF and CVR at Rest and After NTG in Relation to Thallium Uptake Pattern

MBF and CVR at rest and after NTG in relation to rest-redistribution ^{201}Tl SPECT findings are illustrated in Figures 2 and 3, respectively.

In segments of normal ^{201}Tl uptake, MBF significantly decreased after NTG spray (0.91 ± 0.35 to 0.78 ± 0.29 mL/min/g, $P < 0.0001$) (Fig. 2). In contrast, CVR did not change significantly after NTG administration (122 ± 51 to 127 ± 55 mm Hg/[mL/min/g], $P = 0.206$) (Figs. 3 and 4).

MBF tended to increase after NTG spray in the segments with a reversible ^{201}Tl defect despite the decline in perfusion pressure after NTG spray, but the increase was not significant (0.84 ± 0.28 to 0.88 ± 0.22 mL/min/g, $P = 0.395$) (Fig. 2). MBF did not significantly change in segments with a mild-to-moderate irreversible ^{201}Tl defect (0.66 ± 0.27 to 0.64 ± 0.22 mL/min/g, $P = 0.917$). Notably, CVR showed a significant reduction after NTG in segments with a reversible ^{201}Tl defect (141 ± 50 to 114 ± 29 mm Hg/[mL/min/g], $P = 0.004$) (Figs. 3 and 4) and in those with a mild-to-moderate irreversible ^{201}Tl defect (165 ± 64 to 149 ± 60 mm Hg/[mL/min/g], $P = 0.003$) (Fig. 3).

In the segments with a severe irreversible ^{201}Tl defect, NTG decreased MBF (0.52 ± 0.17 to 0.42 ± 0.07 mL/min/g, $P = 0.024$) (Fig. 3) without changing CVR (215 ± 47 to 230 ± 20 mm Hg/[mL/min/g], $P = 0.297$) (Fig. 4).

DISCUSSION

The current results indicate that NTG does not necessarily increase global or regional MBF in the absolute term in patients with coronary artery disease or in healthy volunteers. However, NTG preferentially reduces CVR in regions with a reversible ^{201}Tl defect or in those with a mild-to-moderate irreversible ^{201}Tl defect, without changing CVR in

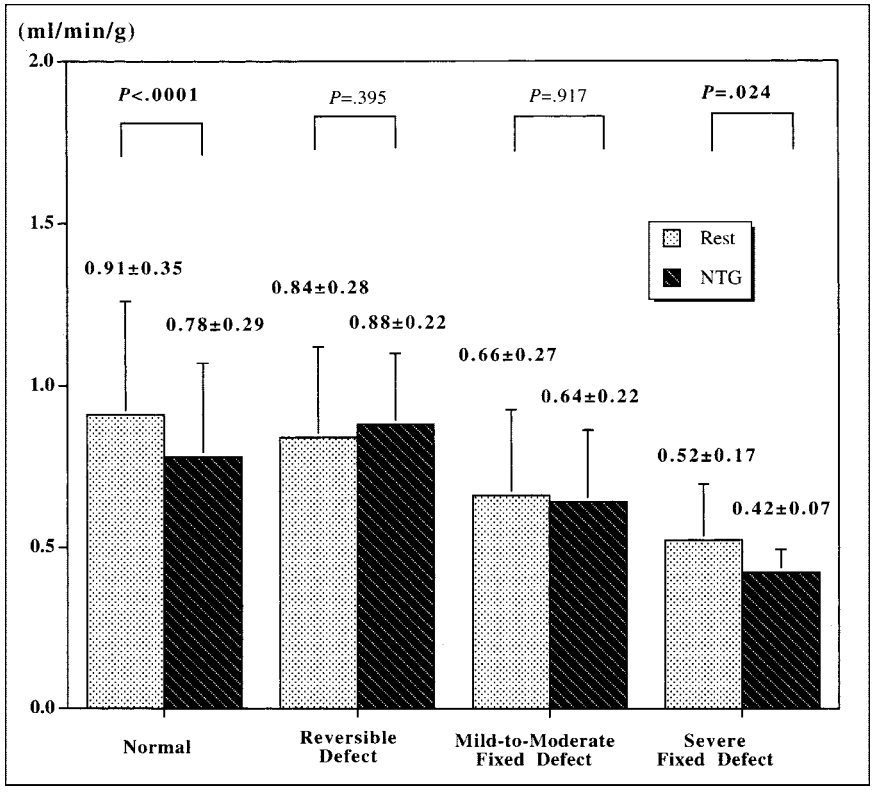

FIGURE 2. MBF at rest and after NTG, compared with rest-redistribution ^{201}Tl SPECT findings.

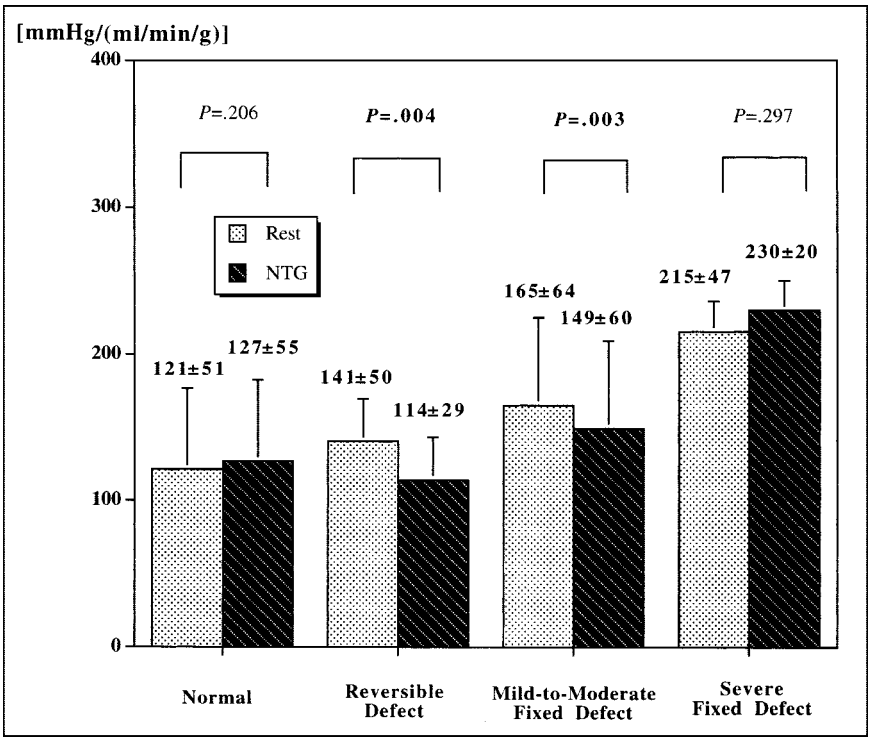

FIGURE 3. CVR at rest and after NTG, compared with rest-redistribution ^{201}Tl SPECT findings.

segments with normal ^{201}Tl activity or in segments with a severe irreversible ^{201}Tl defect.

It is well known that NTG relieves anginal pain in patients with coronary artery disease. It has been observed that NTG dilates the epicardial coronary artery (*30*,*31*), especially at sites of stenosis (*31*), and collateral vessels (*32*) on coronary angiography. However, there is a controversy over the effect of NTG on MBF. The proposed mechanism of action of NTG in the relief of angina pectoris involves 2 types of effects: redistribution of coronary blood flow (*33*,*34*), and a decrease in the myocardial oxygen requirement though changing the preload and afterload without significantly changing flow (*35–37*). Currently, PET is considered one of the most reliable noninvasive methods to assess regional MBF (*21*,*24*,*26–29*,*34*). However, few studies have investigated the effect of NTG on MBF using PET (*34*).

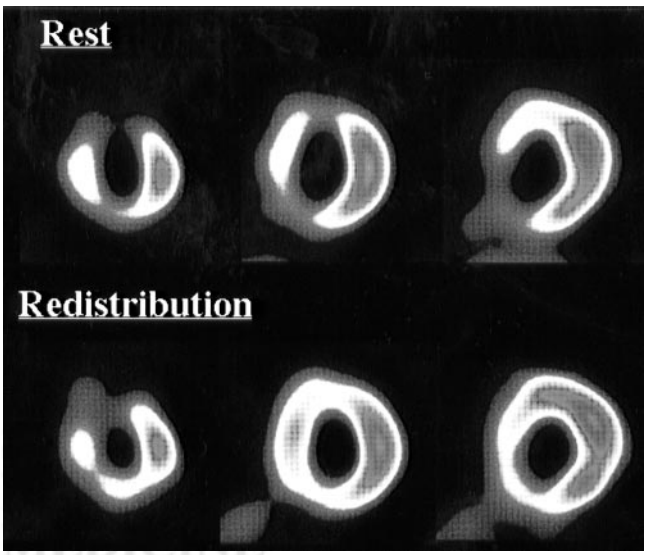

FIGURE 4. Short-axis images of rest and redistribution ^{201}Tl SPECT for patient who shows reversible perfusion defects in anterior and septal regions. In midventricular septum, CVR decreased after NTG spray from 151 to 126 mm Hg/(mL/min/g), whereas CVR did not significantly change in lateral wall with normal ^{201}Tl activity (130 vs. 132 mm Hg/[mL/min/g]).

In our observations, neither global MBF nor RPP-normalized global MBF was significantly altered after NTG in the patients or in the healthy volunteers (Table 2), and these findings agree well with those of the previous reports (*34*,*35*). Thus, NTG is considered to have little effect on global left ventricular circulation. In terms of regional MBF, Horwits et al. reported that NTG improved perfusion in regions of ischemic myocardium in a study using direct intramyocardial injection of an inert radioactive gas to measure regional myocardial circulation (*33*). In addition, Fallen et al. demonstrated that NTG altered MBF, preferentially increasing the blood flow to areas of reduced perfusion with little effect on global MBF, using PET and ^{13}N ammonia (*34*). In the current study, however, NTG did not significantly increase MBF in the ischemic segments (Fig. 2). This difference may be attributed to the difference in hemodynamic response to nitrates. In the studies cited above, NTG did not significantly change blood pressure or heart rate (*33*,*34*). In the current study, however, NTG spray significantly reduced arterial blood pressure. Thus, the difference in regional MBF response to NTG is thought to be

related to the difference in coronary perfusion pressure after NTG. However, we have observed that NTG preferentially reduced CVR in segments with a reversible ^{201}Tl defect or those with a mild-to-moderate irreversible ^{201}Tl defect, without changing CVR in segments with normal ^{201}Tl uptake (Fig. 3). In addition, the COV of MBF decreased significantly after NTG spray in patients. Therefore, the current findings do not contradict the results of previous studies indicating that NTG redistributes coronary blood flow from the nonischemic to the ischemic region (*33*,*34*).

Recently, several investigations suggested the effectiveness of NTG for the evaluation of myocardial viability and prognosis (*13–20*). Rest-redistribution ^{201}Tl imaging has been considered a method of choice for viability assessment (*1*,*2*,*4–6*,*12*). According to various reports, segments with an irreversible severe reduction of ^{201}Tl activity were generally considered nonviable, whereas all other segments were considered viable (*1*,*2*,*4*,*6*). Myocardial segments with a reversible ^{201}Tl defect or those with a mild-to-moderate irreversible ^{201}Tl defect are considered viable myocardium with ischemia (*6*). In addition, regions with normal ^{201}Tl uptake are considered nonischemic. In the present study, NTG preferentially reduced CVR in these viable myocardial segments with ischemia (Figs. 3 and 4). On the other hand, it did not change CVR in the nonischemic myocardium (Figs. 3 and 4) or the nonviable myocardium (Fig. 3). The change in vascular tone caused by NTG has reduced the flow disparity in the viable myocardium (regions with normal ^{201}Tl uptake, those with a reversible ^{201}Tl defect, and those with a mild-to-moderate irreversible ^{201}Tl defect), preserving the flow difference between the viable and the nonviable myocardium (regions with severe irreversible ^{201}Tl defect) (Fig. 2). In other words, the changes of CVR caused by NTG will relatively augment flow tracer uptake in the viable myocardium with ischemia, compared with that in the nonischemic or the nonviable myocardium. Thus, administration of a myocardial perfusion tracer after the load of nitrates is considered to be an effective approach to identify viable myocardium.

The reduction in CVR in the viable myocardium with ischemia could be caused by the dilatation of epicardial coronary stenosis (*31*) and the collateral vessels (*32*). However, CVR in the nonviable myocardium might not be reduced, probably because of damage in the myocardium itself or the microcirculation, despite the dilatation of these vessels. On the other hand, CVR in the nonischemic myocardium may mainly be determined by the small microvessels, on which NTG has little effect (*38*).

The current study has some limitations. First, the patient population is not typical for viability assessment. Many patients had preserved left ventricular function. Second, a ^{201}Tl rest-redistribution study is not an ideal reference standard for viability assessment. In addition, no attenuation correction was performed for the ^{201}Tl data. Regional ^{201}Tl uptake was not compared with a normal database, possibly leading to a misclassification of some viable segments. However, many of the studies have used the single threshold value and have obtained clinically satisfactory results (*4*,*6*). Thus, it is unlikely that the use of a single threshold value would have substantially affected our results. Finally, the modality and dosage of nitrate administration could have had some influence on the results.

CONCLUSION

NTG does not necessarily increase global or regional absolute MBF in patients with coronary artery disease or in healthy volunteers. However, NTG preferentially decreased CVR in the viable myocardium with ischemia without altering CVR in nonischemic or nonviable myocardium. The changes in CVR caused by NTG will relatively increase flow tracer uptake in viable myocardium with ischemia, in comparison with flow tracer uptake in nonischemic or nonviable myocardium. Thus, administration of a flow tracer after NTG is considered effective in identifying viable myocardium.

ACKNOWLEDGMENTS

We thank Keiichi Matsumoto; Tohru Fujita; Haruhiro Kitano; Takahiro Mukai, PhD; and the cyclotron staff for their expert technical assistance. We acknowledge Tadashi Ikeda, MD, for assistance with clinical data.

REFERENCES

1. Dilsizian V, Perrone-Filardi P, Arrighi JA, et al. Concordance and discordance between stress-redistribution-reinjection and rest-redistribution thallium imaging for assessing viable myocardium: comparison with metabolic activity by positron emission tomography. *Circulation.* 1993;88:941–952.
2. Ragosta M, Beller GA, Watson DD, Kaul S, Gimple LW. Quantitative planar rest-redistribution ^{201}Tl imaging in detection of myocardial viability and prediction of improvement in left ventricular function after coronary bypass surgery in patients with severely depressed left ventricular function. *Circulation.* 1993;87:1630–1641.
3. Udelson JE, Coleman PS, Metherall J, et al. Predicting recovery of severe regional ventricular dysfunction: comparison of resting scintigraphy with ^{201}Tl and ^{99m}Tc-sestamibi. *Circulation.* 1994;89:2552–2561.
4. Perrone-Filardi P, Pace L, Prastaro M, et al. Dobutamine echocardiography predicts improvement of hypoperfused dysfunctional myocardium after revascularization in patients with coronary artery disease. *Circulation.* 1995;91:2556–2565.
5. Sansoy V, Glover DK, Watson DD, et al. Comparison of thallium-201 resting redistribution with technetium-99m-sestamibi uptake and functional response to dobutamine for assessment of myocardial viability. *Circulation.* 1995;92:994–1004.
6. Perrone-Filardi P, Pace L, Prastaro M, et al. Assessment of myocardial viability in patients with chronic coronary artery disease: rest-4-hour-24-hour ^{201}Tl tomography versus dobutamine echocardiography. *Circulation.* 1996;94:2712–2719.
7. Pierard LA, Lancellotti P, Benoit T. Myocardial viability: stress echocardiography vs nuclear medicine. *Eur Heart J.* 1997;18(suppl D):D117–D123.
8. Gunning MG, Anagnostopoulos C, Knight CJ, et al. Comparison of ^{201}Tl, ^{99m}Tc-tetrofosmin, and dobutamine magnetic resonance imaging for identifying hibernating myocardium. *Circulation.* 1998;98:1869–1874.
9. Narula J, Dawson MS, Singh BK, et al. Noninvasive characterization of stunned, hibernating, remodeled and nonviable myocardium in ischemic cardiomyopathy. *J Am Coll Cardiol.* 2000;36:1913–1919.
10. La Canna G, Rahimtoola SH, Visioli O, et al. Sensitivity, specificity, and predictive accuracies of non-invasive tests, singly and in combination, for diagnosis of hibernating myocardium. *Eur Heart J.* 2000;21:1358–1367.
11. Gunning MG, Kaprielian RR, Pepper J, et al. The histology of viable and hibernating myocardium in relation to imaging characteristics. *J Am Coll Cardiol.* 2002;39:428–435.

12. Bax JJ, Maddahi J, Poldermans D, et al. Sequential ^{201}Tl imaging and dobutamine echocardiography to enhance accuracy of predicting improved left ventricular ejection fraction after revascularization. *J Nucl Med.* 2002;43:795–802.
13. He ZX, Darcourt J, Guignier A, et al. Nitrates improve detection of ischemic but viable myocardium by thallium-201 reinjection SPECT. *J Nucl Med.* 1993;34: 1472–1477.
14. Bisi G, Sciagra R, Santoro GM, et al. Rest technetium-99m sestamibi tomography in combination with short-term administration of nitrates: feasibility and reliability for prediction of postrevascularization outcome of asynergic territories. *J Am Coll Cardiol.* 1994;24:1282–1289.
15. Maurea S, Cuocolo A, Soricelli A, et al. Enhanced detection of viable myocardium by technetium-99m-MIBI imaging after nitrate administration in chronic coronary artery disease. *J Nucl Med.* 1995;36:1945–1952.
16. He ZX, Medrano R, Hays JT, et al. Nitroglycerin-augmented ^{201}Tl reinjection enhances detection of reversible myocardial hypoperfusion: a randomized, double-blind, parallel, placebo-controlled trial. *Circulation.* 1997;95:1799–1805.
17. Sciagrà R, Bisi G, Santoro GM, et al. Comparison of baseline-nitrate technetium-99m sestamibi with rest-redistribution thallium-201 tomography in detecting viable hibernating myocardium and predicting postrevascularization recovery. *J Am Coll Cardiol.* 1997;30:384–391.
18. Basu S, Senior R, Raval U, et al. Superiority of nitrate-enhanced ^{201}Tl over conventional redistribution ^{201}Tl imaging for prognostic evaluation after myocardial infarction and thrombolysis. *Circulation.* 1997;96:2932–2937.
19. Sciagra R, Pellegri M, Pupi A, et al. Prognostic implications of Tc-99m sestamibi viability imaging and subsequent therapeutic strategy in patients with chronic coronary artery disease and left ventricular dysfunction. *J Am Coll Cardiol.* 2000;36:739–745.
20. Sciagra R, Leoncini M, Marcucci G, Dabizzi RP, Pupi A. Technetium-99m sestamibi imaging to predict left ventricular ejection fraction outcome after revascularisation in patients with chronic coronary artery disease and left ventricular dysfunction: comparison between baseline and nitrate-enhanced imaging. *Eur J Nucl Med.* 2001;28:680–687.
21. Tadamura E, Iida H, Matsumoto K, et al. Comparison of myocardial blood flow during dobutamine-atropine infusion with that after dipyridamole administration in normal men. *J Am Coll Cardiol.* 2001;37:130–136.
22. Tadamura E, Kudoh T, Motooka M, et al. Assessment of regional and global left ventricular function by reinjection T1–201 and rest Tc-99m sestamibi ECG-gated SPECT: comparison with three-dimensional magnetic resonance imaging. *J Am Coll Cardiol.* 1999;33:991–997.
23. Tadamura E, Kudoh T, Motooka M, et al. Use of technetium-99m sestamibi ECG-gated single-photon emission tomography for the evaluation of left ventricular function following coronary artery bypass graft: comparison with three-dimensional magnetic resonance imaging. *Eur J Nucl Med.* 1999;26:705–712.
24. Baliga RR, Rosen SD, Camici PG, et al. Regional myocardial blood flow redistribution as a cause of postprandial angina pectoris. *Circulation.* 1998;97: 1144–1149.
25. Germano G, Kiat H, Kavanagh PB, et al. Automatic quantification of ejection fraction from gated myocardial perfusion SPECT. *J Nucl Med.* 1995;36:2138–2147.
26. Iida H, Rhodes C, de Silva R, et al. Use of the left ventricular time-activity curve as a noninvasive input function in dynamic oxygen-15-water positron emission tomography. *J Nucl Med.* 1992;33:1669–1677.
27. Iida H, Kanno I, Takahashi A, et al. Measurement of absolute myocardial blood flow with $H_2{}^{15}O$ and dynamic positron-emission tomography: strategy for quantification in relation to the partial-volume effect. *Circulation.* 1988;78:104–115.
28. Laine H, Raitakari OT, Niinikoski H, et al. Early impairment of coronary flow reserve in young men with borderline hypertension. *J Am Coll Cardiol.* 1998; 32:147–153.
29. Kofoed KF, Czernin J, Johnson J, et al. Effects of cardiac allograft vasculopathy on myocardial blood flow, vasodilatory capacity, and coronary vasomotion. *Circulation.* 1997;95:600–606.
30. Feldman RL, Pepine CJ, Curry RC Jr, et al. Coronary arterial responses to graded doses of nitroglycerin. *Am J Cardiol.* 1979;43:91–97.
31. Brown BG, Bolson E, Petersen RB, Pierce CD, Dodge HT. The mechanisms of nitroglycerin action: stenosis vasodilatation as a major component of the drug response. *Circulation.* 1981;64:1089–1097.
32. Fujita M, Yamanishi K, Inoko M, et al. Preferential dilation of recipient coronary arteries of the collateral circulation by intracoronary administration of nitroglycerin. *J Am Coll Cardiol.* 1994;24:631–635.
33. Horwitz LD, Gorlin R, Taylor WJ, et al. Effects of nitroglycerin on regional myocardial blood flow in coronary artery disease. *J Clin Invest.* 1971;50:1578–1584.
34. Fallen EL, Nahmias C, Scheffel A, Coates G, Beanlands R, Garnett ES. Redistribution of myocardial blood flow with topical nitroglycerin in patients with coronary artery disease. *Circulation.* 1995;91:1381–1388.
35. Gorlin R, Brachfeld N, MacLeod C, et al. Effect of nitroglycerin on the coronary circulation in patients with coronary artery disease or increased left ventricular work. *Circulation.* 1959;19:705–718.
36. Bernstein L, Friesinger GC, Lichtlen PR, et al. The effect of nitroglycerin on the systemic and coronary circulation in man and dogs: myocardial blood flow measured with xenon. *Circulation.* 1966;33:107–116.
37. Lahiri A, Crawley JC, Sonecha TN, Raftery EB. Acute and chronic effects of sustained action buccal nitroglycerin in severe congestive heart failure. *Int J Cardiol.* 1984;5:39–48.
38. Marcus ML, Chilian WM, Kanatsuka H, Dellsperger KC, Eastham CL, Lamping KG. Understanding the coronary circulation through studies at the microvascular level. *Circulation.* 1990;82:1–7.